Mechanics of Materials 165 (2022) 104156

Contents lists available at ScienceDirect

Mechanics of Materials

journal homepage: www.elsevier.com/locate/mecmat

Research paper

Multiscale modeling of materials: Computing, data science, uncertainty and goal-oriented optimization

Nikola Kovachki[1], Burigede Liu[1], Xingsheng Sun[1], Hao Zhou[1], Kaushik Bhattacharya *, Michael Ortiz, Andrew Stuart

California Institute of Technology, United States of America

ARTICLE INFO

Keywords:
Multiscale modeling
Materials by design
Machine learning
Uncertainty quantification

ABSTRACT

The recent decades have seen various attempts at accelerating the process of developing materials targeted towards specific applications. The performance required for a particular application leads to the choice of a particular material system whose properties are optimized by manipulating its underlying microstructure through processing. The specific configuration of the structure is then designed by characterizing the material in detail, and using this characterization along with physical principles in system level simulations and optimization. These have been advanced by multiscale modeling of materials, high-throughput experimentations, materials data-bases, topology optimization and other ideas. Still, developing materials for extreme applications involving large deformation, high strain rates and high temperatures remains a challenge. This article reviews a number of recent methods that advance the goal of designing materials targeted by specific applications.

1. Introduction

The development of new materials guided by the process-structure-properties-performance paradigm has been the core endeavor of materials science, while the design and optimization of machines by using physical principles and materials characterization have been the core endeavor of mechanical and structural engineering. These have gradually merged as we seek to develop materials focused on particular applications, especially those involving extreme conditions. A general framework has emerged and this is described in Fig. 1.

We seek to design an application ("1" in Fig. 1) with a particular material system ("2" in Fig. 1). In the established approach of mechanical design, we characterize the material system with a constitutive relation ("3" in Fig. 1) and use it along with physical principles (balance laws) to design and optimize an application. The constitutive relation is intuited from experiments to characterize the material system ("4" in Fig. 1), qualitative knowledge from lower scale physics ("5" in Fig. 1), symmetry, ease of implementation, history and other considerations. Multiscale modeling of materials seeks to make the connection to lower scale models stronger. The lower scale models are built on the basis of additional experiments at that scale and even lower scale models. And so on. Thus, the modeling of materials results in a complex cascade of models at different scales addressing different phenomena at different levels of fidelity. The material system is itself developed and optimized through a series of experiments ("6" in Fig. 1) and process models ("7" in Fig. 1). The process models may also have their own multiscale cascade.

While this conceptual framework is widely used, the detailed implementation requires expert judgement and decisions due to limitations in the amount of data that is available, limitations in the theoretical and modeling tools and the prohibitive computational cost of a brute force implementation. *The goal of this paper is to review recent work that provides ideas and tools to implement and exploit this framework for rapidly developing and optimizing materials for particular applications*.

Underlying the framework described above is the observation that the macroscopic behavior of materials is the end result of a number of mechanisms that operate across a broad range of disparate scales (Phillips, 2001). The paradigm of multiscale modeling seeks to address this complexity using a 'divide and conquer' approach shown in Fig. 2 (Ortiz et al., 2001; Fish, 2009; de Borst and Ramm, 2011; Van Der Giessen et al., 2020). The complex range of material behavior is first divided into an ordered hierarchy of scales, the relevant mechanisms at each scale are identified and analyzed using theories/tools based on an individual scale, and the hierarchy is put back together by passing information between scales. Importantly, the passage of information between scales is pair-wise, with the larger-scale model both regulating (through average kinematic constraints

* Corresponding author.
E-mail address: bhatta@caltech.edu (K. Bhattacharya).
[1] These authors have contributed equally.

https://doi.org/10.1016/j.mechmat.2021.104156
Received 12 April 2021; Received in revised form 10 November 2021; Accepted 11 November 2021
Available online 27 November 2021

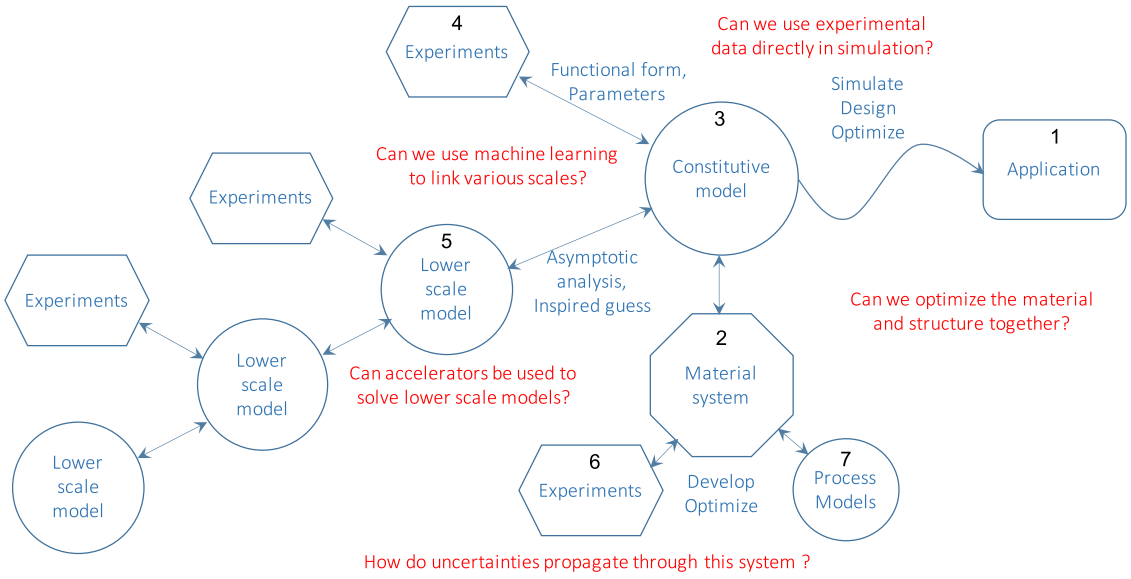

Fig. 1. The framework of application-driven materials by design.

like the boundary conditions) and averaging (the dynamic response like the stress) the smaller-scale model. The mathematical theory of homogenization (Bensoussan et al., 2011; Pavliotis and Stuart, 2008) provides a concrete basis in specialized situations, but the underlying conceptual framework is widely used.

The computational implementation of this framework requires the repeated solution of the models at individual scales. Recent computing platforms complement the central processing units (CPUs) with massively parallel accelerators like graphics processing units (GPUs) (Kirk and Hwu, 2016; Kothe et al., 2019). Such accelerators contain thousands of processors, but these are not independent. Instead, they are grouped together in 'warps' that share a memory and execute the same instructions but on possible different data (SIMD). Consequently, they can provide enormous computational power if the calculations are carefully arranged to meet the limitations of the architecture. This raises the first question: *Can we use accelerators to efficiently and rapidly solve models at the individual scales?* Section 3 reviews recent work of Zhou and Bhattacharya (2021) that describes how such accelerators can be effectively used in the solution of problems of micromechanics. A key idea in this work is to note that nonlinear partial differential equations that describe micromechanical phenomena come about through a *composition* of universal laws of physics (kinematic compatibility and balance of mass, momenta, energy etc.) and the particular constitutive models of the material under study. The former are nonlocal, but may be interpreted as projections in appropriate function space. The material behavior is nonlinear and may involve time derivatives, but is spatially *local*. Thus each step is amenable to efficient implementation in accelerators.

We then turn to the issue of bridging two scales. In the multiscale paradigm, the behavior of each point at each instant of time in the larger scale model has to be informed by a solution of the smaller scale model. This idea is implemented directly in the concurrent multiscale approaches like FE^2 (Feyel and Chaboche, 2000). Unfortunately this is prohibitively expensive especially if one has to study multiple scales. So, a widely used approach is sequential multiscale or parameter passing method where the form of the larger scale model is postulated and the parameters are evaluated from smaller scale simulations (see Cheng et al., 2019; Fu et al., 2005; Balasubramanian and Anand, 2002 for examples). However, this introduces an additional layer of modeling. All of this leads to the question: *Can we use use techniques from machine learning, such as Gaussian processes, deep neural networks or other supervised learning techniques to link scales?* Section 3 reviews the recent work

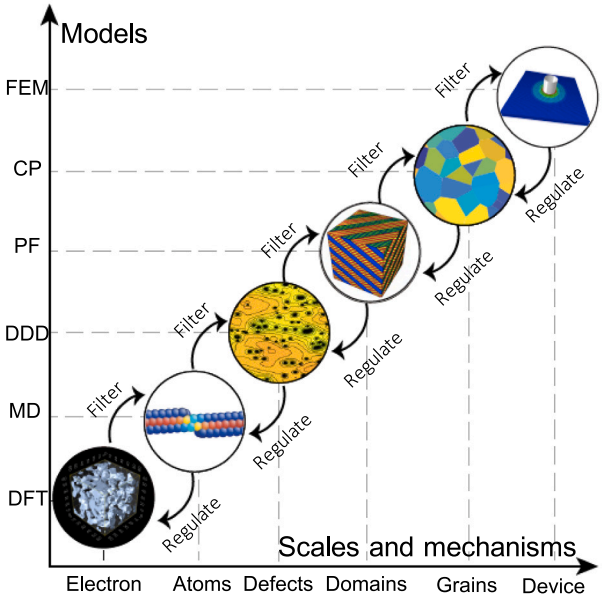

Fig. 2. Multiscale modeling of materials is a 'divide and conquer' approach to describe the complexity of material behavior.

of Liu et al. (2022) that studies the two scale problem of the response of polycrystalline magnesium to impact loading. The key idea is to view the lower-scale model (a polycrystalline ensemble described by crystal plasticity augmented to include twinning in this case) as a map from a strain history to a stress history, and to approximate this map using a combination of model reduction and machine learning (Bhattacharya et al., 2021).

Section 5 describes an alternative approach to bridging scales where the results of the micro-scale simulations are used directly in macro-scale simulations without the introduction of any empirical or machine-learnt models. This approach was initially developed with the goal of directly using experimental observations in simulations without any constitutive models (Kirchdoerfer and Ortiz, 2016, 2017, 2018). The emergence of full-field diagnostic methods like digital image correlation (McCormick and Lord, 2010) and high energy x-ray diffraction

microscopy (Schwartz et al., 2009) has created a new environment that is rich in experimental data. This motivates a new question: *Can we use experimental data directly in computations without the use of any constitutive models?* The approach seeks to find those stress and strain fields that satisfy the laws of physics (kinematic compatibility and equilibrium) and whose local relationship best approximates the available data. Section 5 shows how this approach can be extended to multi-scale modeling and describes the work of Karapiperis et al. (2021) in granular media.

The complexity of the material response leads to uncertainty, and this uncertainty is often the main source of uncertainty in engineering applications. Therefore, it is important to quantify the integral uncertainties across the various scales in order to identify adequate design margins for the design. However, the direct estimation of integral material uncertainties is prohibitively expensive. This leads to the question: *How do uncertainties propagate across scales, and how do we quantify the integral material uncertainty?* Section 6 reviews the recent work of Liu et al. (2021) that provides the bounds on the integral uncertainty of penetration of a rigid impactor through a polycrystalline magnesium plate. The key idea is to exploit the hierarchy of multiscale modeling by viewing the model at each scale as a function and the integral response as a composition of the functions. We can then bound the integral uncertainties using the uncertainty of each individual scale.

A closely related issue is to design materials focussed on particular applications. This in turn requires an understanding of the sensitivity of the integral response to individual mechanisms — for example the sensitivity of the ballistic response to the critical resolved shear stress of a particular slip system. This is not always easy to evaluate, since the mechanism is removed by various scales from the application. The problem of finding sensitivities is closely related to that of quantifying uncertainties, and we can again take advantage of the hierarchical structure of the multiscale model.

Finally, the framework described in Fig. 1 first optimizes the material against some overall measure and then optimizes the configuration in which the material is deployed for a given application. Thermo-mechanical processing of an alloy can control microstructure (grain size, texture and precipitation) which in turn controls the overall properties (toughness and strength). Alloying can also do the same either directly (solution hardening) or indirectly (by controlling microstructure). It has long been recognized that doing so can trade one property to another, and this is done against some composite material metric or Ashby plots depending on the material. The material is then used for the application and the configuration is then optimized. This raises the question: *Can we optimize the material and the structure simultaneously?* Section 7 reviews the work of Sun et al. (2021) that shows that the simultaneous optimization of a bi-material plate can lead to significantly better ballistic performance compared to a sequential optimization. The key idea is that not all parts of a structure perform the same function, and different parts of the structure may have different property requirements.

2. Setting and overview

Multiscale modeling follows a 'divide and conquer' approach where the passage of information between scales is pair-wise as described above. So we consider the situation shown in Fig. 3, noting that the ideas can be extended to multiple scales using this multiscale modeling paradigm. We consider the mechanical setting for specificity. We have a finer *microscopic* scale which we take to be a scale on which the material is heterogeneous (e.g., polycrystals, domain patterns and grains), and a coarser *macroscopic* scale which we take to be the scale of application or device.

Given a domain Ω and some initial and boundary conditions, the *macroscopic problem* is to solve

$$\nabla_x \cdot \bar{S} = \bar{\rho}\bar{u}_{tt} \quad on\ \Omega \tag{1}$$

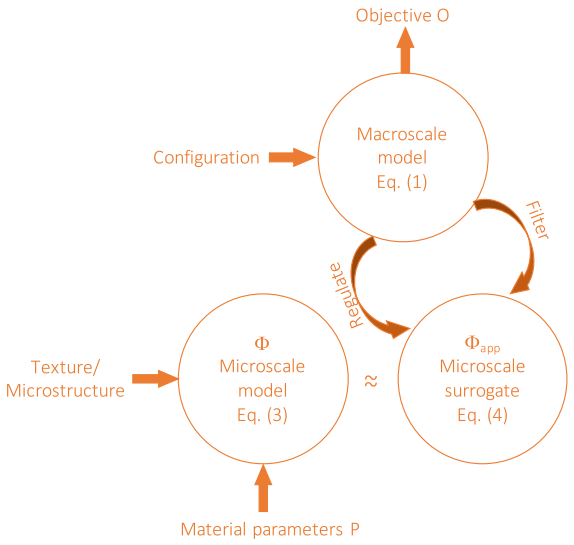

Fig. 3. The general setting.

where $\bar{u} : \Omega \to \mathbb{R}^3$ is the macroscopic deformation and $\bar{S} : \Omega \to \mathbb{R}^{3\times 3}$ is the macroscopic Piola–Kirchhoff stress. To complete the system, we need to specify the macroscopic constitutive relation that is a map from the deformation gradient history to the stress

$$\boldsymbol{\Phi} : \{\bar{F}(x,\tau) : 0 \le \tau \le t\} \to \bar{S}(x,t) \tag{2}$$

at each point x at each instant t.

In the multiscale modeling framework, the map (2) is obtained by solving the *microscopic problem* on a unit cell Y that describes the heterogeneity and some complex physics. In the models of interest, we describe the state of the solid by a microscopic deformation gradient F and a set of microscopic internal variables λ (phase fraction, plasticity, director field, fracture field etc.). In the absence of (micro) inertia, these are governed by a set of coupled equations:

$$\nabla \cdot \big(W_F(\nabla u, \lambda, y; P)\big) = 0, \quad W_\lambda(\nabla u, \lambda, y; P) + D_v(\lambda_t, y; P) = 0 \tag{3}$$

up to time t subject to some initial data and the boundary condition that $u(y,\tau) - \bar{F}(x,t)y$ is periodic so that $\langle F(y,\tau)\rangle = \bar{F}(x,\tau)$. Above, $u : Y \to \mathbb{R}^3$ is the microscopic deformation, $F : Y \to \mathbb{R}^{3\times 3}$ is the microscopic deformation gradient, $\lambda : Y \to \mathbb{R}^d$ is the state variable, internal variable or order parameter, $P \in \mathbb{R}^p$ is a set of material parameters, $W : \mathbb{R}^{3\times 3} \times \mathbb{R}^d \times \Omega \times \mathbb{R}^p \to \mathbb{R}$ is the stored (elastic) energy density, $D : \mathbb{R}^d \times \Omega \times \mathbb{R}^d \to \mathbb{R}$ is the dissipation potential, and $\langle\cdot\rangle$ denotes an average over a unit cell Y. Note that the material properties are heterogeneous at the microscopic scale as a result of microstructure or texture, and this is represented by the fact that the constitutive functions W, D depend explicitly on y. We then obtain $\bar{S}(x,t) = \langle W_F(F(y,t), \lambda(y,t))\rangle$. Note that x and t are parameters in the microscopic problem, and the microscopic problem has to be solved at each point x at each instant t.

Since the macroscopic problem prescribes the boundary condition $\bar{F}$ that solves the microscopic problem, we say that the macroscopic problem *regulates* the microscopic problem. Further, since the microscopic problem returns only the average stress $\bar{S}$, we say that the macroscopic problem also *filters* the results of the microscopic problem.

The direct implementation of this framework — where we actually solve the microscopic problem at point x at each instant t has been called the concurrent or FE^2 approach. While this has been demonstrated in selected examples (e.g., Feyel and Chaboche, 2000), it is generally prohibitively computationally expensive. So it is natural to create a *surrogate* that approximates the microscopic problem

$$\boldsymbol{\Phi}_{\text{app}} \approx \boldsymbol{\Phi}, \tag{4}$$

that is computationally more efficient. The macroscopic problem then interacts with the surrogate of the microscopic problem. The classical approach is to postulate a parametrized macroscopic constitutive model and use data generated by the microscopic model to fit the parameter. However, this is limited in fidelity, especially in complex problems involving microstructure evolution. This has motivated the development of new approaches, and we describe two in this paper. The first, presented in Section 4, uses deep neural networks combined with model reduction as the surrogate, and the surrogate is trained using data generated by repeated solution of the microscopic problem. The second, presented in Section 5, uses the data directly as the surrogate. The methods provide the fidelity of the microscopic problem, but with significantly reduced (online) computational cost. Note that both these methods require repeated solutions of the microscopic problem and Section 3 describes an approach to use GPUs to solve this efficiently. Section 6 seeks to quantify the uncertainties in this framework. We have uncertainties in the microscopic model (specifically the material parameters P and the texture), and we seek to understand the consequence of these uncertainties on the uncertainty in macroscopic performance. This includes the uncertainties created by the introduction of the surrogate. Finally, Section 7 concerns design where we seek to simultaneously optimize the material (represented through the material parameters P and the texture of the microscopic model) and the configuration (domain, multiple materials).

The methods that we present are broadly applicable to phenomena that are described by the framework above. So they are broadly applicable to polymers, metals and granular materials. They have been developed in various contexts, and have been applied to different material systems. This paper seeks to present the interconnections between these various methods and systems.

3. Accelerated computations

Multiscale modeling of materials often requires the repeated solution of models at individual scales. For example, in the two-scale setting described in Section 2, we have to repeatedly solve the microscopic problem (3). This section describes an approach that enables the use of accelerators or graphical processing units (GPUs) to efficiently solve (3), i.e., efficiently compute the map Φ.

As described above, the microscopic problem is typically solved under periodic boundary conditions. So one can exploit fast Fourier transform (FFT) following Moulinec and Suquet (1994). These FFT-based simulations have been effectively applied to a variety of applications (e.g.thermoelasticity (Anglin et al., 2014), elasto-viscoplasticity (Lebensohn and Needleman, 2016), dislocations (Berbenni et al., 2020), piezoelectric materials (Vidyasagar et al., 2017), shape-memory polycrystals (Bhattacharya and Suquet, 2005), and crack prediction of brittle materials (Schneider, 2020)). Various methods to accelerate the convergence of FFT-based methods using Neumann series approximation (Monchiet and Bonnet, 2012; Milton, 2020; Moulinec and Silva, 2014; Milton, 2020) and Fourier–Galerkin method (Vondřejc et al., 2014; Mishra et al., 2016) have been developed.

While much of the focus has been on CPUs, recent work has turned to GPUs in parts of the algorithm (Bertin and Capolungo, 2018; Mihaila et al., 2014; Knezevic and Savage, 2014; Eghtesad et al., 2018). Accelerators like GPUs contain thousands of processors, but these are not independent. Instead, they are grouped together in 'warps' that share a memory and execute the same instructions but on possible different data (SIMD). Consequently, they can provide enormous computational power if the calculations are carefully arranged to meet the limitations of the architecture. This section describes how accelerators like graphical processing units (GPUs) can be effectively used in rapidly solving such problems drawing from Zhou and Bhattacharya (2021).

We adopt an implicit time discretization of (3). We introduce the compatibility condition $F = \nabla u$ as a constraint and treat it using the augmented Lagrangian method (Glowinski, 2015) to obtain the saddle point problem

$$\min_{u^{n+1},\lambda^{n+1}} \max_{\Lambda^{n+1}} \int_\Omega \left(W(F,\lambda,x) + \Delta t\, D\left(\frac{\lambda-\lambda^n}{\Delta t}, x\right) + \Lambda\cdot(\nabla u - F) + \frac{\beta}{2}|\nabla u - F|^2 \right) dx$$

for given $\beta > 0$. This problem could be solved via alternating direction method of multipliers (*ADMM*) (Glowinski, 2015) which is an iterative method.

Given $F^n, \lambda^n, u^n, \Lambda^n$,

- *Step 1: Local problem.* Update F, n by solving at each x

$$W_F(F^{n+1},\lambda^{n+1},x) - \Lambda^n + \beta(\nabla u^n - F^{n+1}) = 0, \tag{5}$$

$$W_\lambda(F^{n+1},\lambda^{n+1},x) + \Delta t \frac{\partial D}{\partial \lambda}\left(\frac{\lambda^{n+1}-\lambda^n}{\Delta t}, x\right) = 0. \tag{6}$$

- *Step 2: Helmholtz projection.* Update u by solving $-\Delta u^{n+1} = \nabla\cdot\left(-F^{n+1} + \frac{1}{\beta}\Lambda^n\right)$.
- *Step 3: Update Lagrange multiplier.* Update Λ as $\Lambda^{n+1} = \Lambda^n + \beta(\nabla u^{n+1} - F^{n+1})$.
- *Step 4: Check for convergence.* Check both primal and dual feasibility:

$$r_p := \|\nabla u^i - F^i\|_{L^2} \le r_p^{\text{tolerance}}, \quad r_d := \beta\|\nabla u^{i+1} - \nabla u^i\|_{L^2} \le r_d^{\text{tolerance}} \tag{7}$$

for given $r_p^{\text{tolerance}}, r_d^{\text{tolerance}}$.

This method is known to converge under suitable hypothesis on W, D for all β sufficiently large (Boyd et al., 2011). Step 1 is a local problem, and can be solved trivially in parallel. Note that it is necessary to solve for F^{n+1}, λ^{n+1} accurately in some L^p, thus we can have poor convergence of a small number of points. Therefore, the iterations of all points are not impeded by the poor convergence of a few isolated points. Step 2 leads to a *universal* Poisson's equation for which there are a number of effective parallel solvers. Step 3 is a trivial local update, and step 4 a simple check. Thus, this iterative algorithm can be implemented effectively using accelerators like GPUs as we presently demonstrate. This iterative method also has a close connection to the physics. Step 1 is the constitutive update with the Lagrange multiplier converging to the stress, Step 2 is the compatibility equation with the primal convergence in r_p while the dual convergence in r_d is equivalent to the equilibrium condition.

We apply the method on two separate problems — see Ocegueda and Bhattacharya, 2021 for an application to combined twinning and slip in magnesium. We start with a problem of finite deformation that involves a bifurcation and has been previously studied using finite element method (Triantafyllidis et al., 2006). Consider a 2D periodic inclusion of compliant circular particles in a stiff matrix with the unit cell shown in Fig. 4(a). Both materials are modeled as compressible Mooney–Rivlin materials. As this composite is compressed equibiaxially, it develops a period doubling instability shown in Fig. 4(c). The stress–stretch relation shows the bifurcation in Fig. 4(d). All results are consistent with previous FE simulations. We also use this example to discuss convergence and scaling.

The second concerns liquid crystal elastomers (LCEs). These are rubber-like solids where nematic mesogens are incorporated into the polymer chains. The LCE has a spontaneous or stress-free deformation F depending on the mesogens orientation n, which is a reorientable unit vector. Therefore, the problem has coupled fields with non-convex energy.

Recent experiments have suggested a peculiar behavior in LCEs. When a sheet is stretched in planar extension (PE) where one in-plane direction is stretched while the other is held fixed ($\lambda_x > 1, \lambda_y = 1$), the nominal stress in the stretched direction is smaller than that in

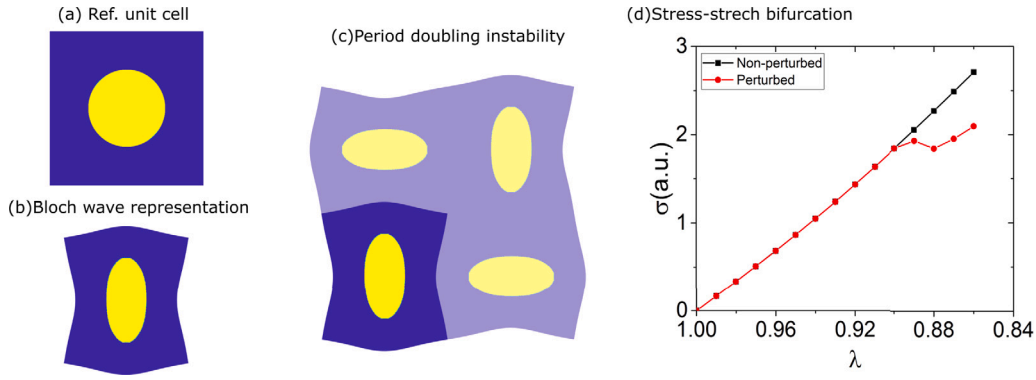

Fig. 4. Bifurcation in nonlinear elastic composite. (a) Unit cell with soft inclusion (yellow) in a hard matrix (blue). (b) Bloch wave instability at $\lambda = 0.89$. (c) The period doubling instability on 2×2 unit cells. (d) Stress–stretch curves with and without instability. (For interpretation of the references to color in this figure legend, the reader is referred to the web version of this article.)

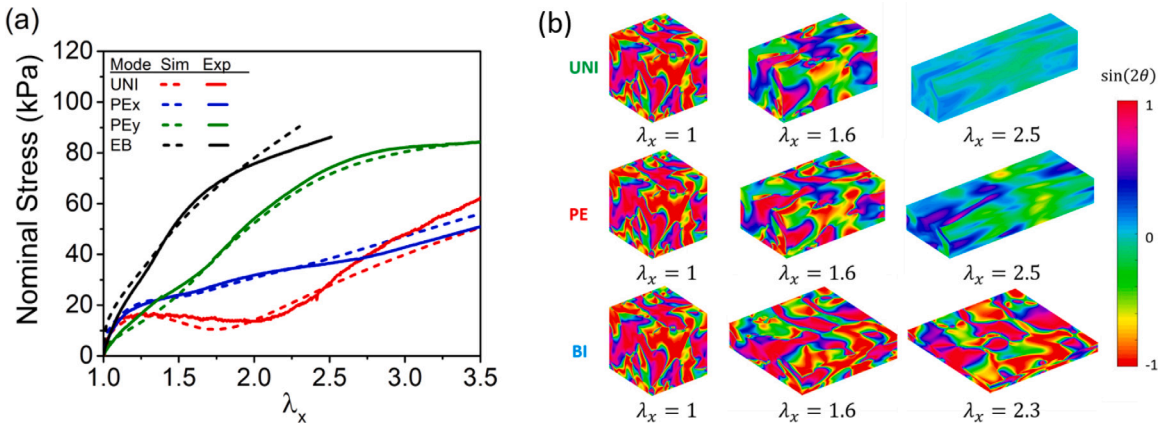

Fig. 5. Unusual behavior of polydomain liquid crystal elastomers. (a) Nominal stress versus stretch under different loading conditions. (b) Microstructure evolution. (θ is the angle of n with x-axis).

the unstretched direction. Fig. 5(a) shows the measured and computed stress–strain curves under uniaxial extension (U), PE and equibiaxial extension (EB) while Fig. 5(b) shows how the directors evolve. Note that the simulations reproduce the complex observed behavior with a few parameters. More importantly, the simulations revealed that the microstructure evolves in such a way in PE that the in-plane shear was always zero, and this is the reason for the observed unusual behavior. Other complex loading protocols also reveal good agreement. Further, the statistics of microstructure evolution measured through X-ray scattering agrees well with the simulations. In short, these simulations provide unique insight into microstructure evolution in LCEs.

The numerical performance and the scaling is demonstrated using the example of the elastic composite in Fig. 6. First, the convergence with mesh is investigated. Taking the finest mesh as the reference, we calculate the relative error (L_2 norm) of deformation gradient, stress and displacement with different mesh size. They converge with a convergence rate of 1.83, 1.84 and 2.15 respectively, close to the theoretically expected value of 2. Turning now to the scaling, we observe a steady decrease of wall time with increased threads of GPU. The slope is fitted as -0.73, suggesting very good scalability of the algorithm. However, it is not perfect (-1) since FFT does not scale perfectly. The scaling is also confirmed by weak scaling. The same configuration is studied using different mesh with proportional threads. Overall, the algorithm and GPU implementation show a good parallel efficiency as the system grows.

4. Machine-learning material behavior

In this section, we describe an approach that uses machine-learning to create a high-fidelity computationally efficient surrogate Φ_{app} of the microscopic model Φ. Machine-learning and especially deep neural networks have been extremely successful in image recognition (LeCun et al., 1995; He et al., 2016) and natural language processing tasks (Goldberg, 2017; Collobert and Weston, 2008). There is also a growing literature on the use of these methods in materials science (Kalidindi and De Graef, 2015). Machine learning has been combined with theoretical calculations, combinatorial synthesis, and high throughput characterization to rapidly identify materials with desired properties (Ludwig, 2019; Umehara et al., 2019; Jain et al., 2013). It has also been applied to parameter passing (Marchand et al., 2020; Cole et al., 2020; Wen and Tadmor, 2019) and to the inversion of experimental data (De Graef, 2020; Chen and Daly, 2018). Image classification and natural language processing have been applied to approximate material constitutive behavior (Le et al., 2015; Mozaffar et al., 2019; Jordan et al., 2020) and homogenization of material behavior (Liu et al., 2019d; Xiao et al., 2019).

A critical challenge in the application of machine learning is that material models like the microscopic model (3) are described as partial differential equations (e.g. equilibrium and evolution equations in our setting) that map inputs from one function space (correspondingly, average strain history) to outputs on another function space (correspondingly, the stress response). However, typical neural network architectures approximate finite dimensional inputs to finite dimensional outputs. So a direct application makes the network dependent on the discretization which introduces artifacts and does not allow us to collect data from diverse sources. One approach to overcome this is shown in Fig. 7 and combines model reduction and neural networks for high-fidelity discretization-independent approximations of maps between function spaces (Bhattacharya et al., 2021). Briefly,

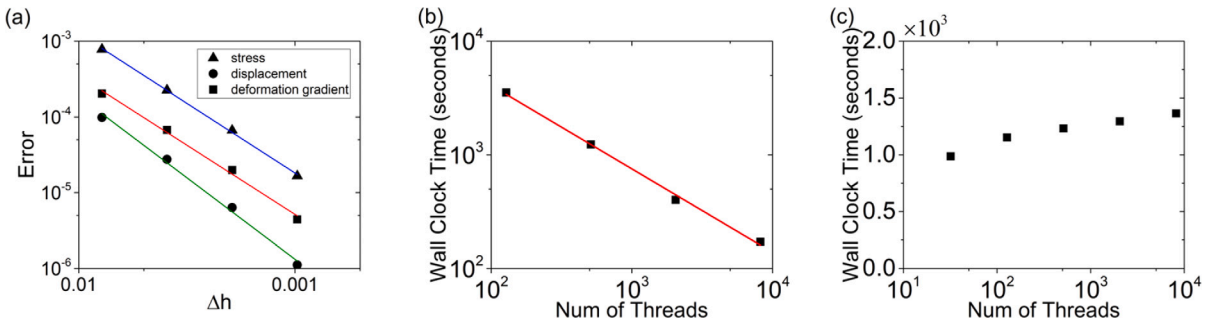

Fig. 6. Performance of accelerated computing. (a) Relative error of physical quantities versus mesh size. (b) Strong scaling. (c) Weak scaling.

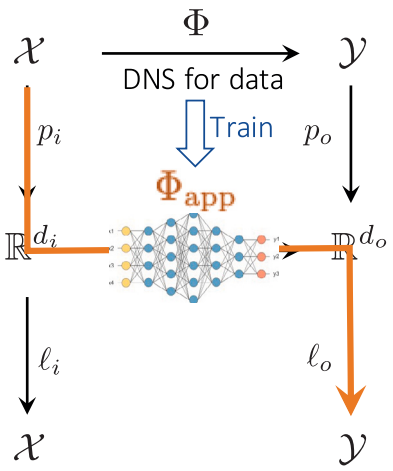

Fig. 7. Architecture for the machine learnt surrogate combines model reduction and deep neural networks.

we build an approximation of an identity map from a function space to itself by a composition of a model reduction map that maps from the function space to a finite dimensional space of latent variables and a lifting map that maps the finite dimensional space to the function space. Examples of such maps are principal component analysis (PCA) and auto-encoders. We implement this map to both the input and output spaces, and a neural network approximation between the finite-dimensional representations (latent variables). The surrogate is a composition of the model reduction map in input space, the neural network approximation and lifting map to output space, and trained using data by the direct numerical simulation of the microscopic problem. Importantly we are able to control this approximation in elliptic partial differential equations with theorems that bound the error in terms of the reduced dimensions, neural network features and training data; similar results are to be expected for parabolic problems. Other approaches of machine learned approximations to the solution operator are explored in Li et al. (2020, 2021).

We have demonstrated the approach to the problems of impact of polycrystalline magnesium in Fig. 8 (Liu et al., 2022). High fidelity crystal plasticity unit cell calculations were used to create a machine learned surrogate that accurately predicts the material response against various strain histories (e.g. Fig. 8(a, b)). The surrogate is implemented as the material model (VUMAT) in the macroscopic solver (ABAQUS) to the study of a plate being impacted with a rigid, massive impactor Fig. 8(c). Once trained, the same surrogate can be used for a range of calculations including the design study on plate thickness (Fig. 8)(d) which shows a change of deformation mode from one dominated by bending to one dominated by punching as well as the Taylor anvil test. Importantly, a representative calculation takes 2362 s, a few times larger than 262 s required for a similar calculation using an empirical constitutive relation (Johnson–Cook) and orders of magnitude smaller than 3.9×10^8 seconds required for a concurrent calculation. Furthermore, the calculation has all the physics of the concurrent calculation. The one-time off-line cost of generating data (5.9×10^6) and training (6.0×10^4) are also smaller than a single concurrent calculation.

5. Data-driven multiscale modeling

In this section, we describe an approach that uses data $D = \{(\bar{F}_i(t), \bar{S}_i(t)) : \bar{S}_i(t) = \Phi(\bar{F}_i(t)), i = 1, \dots, N\}$ obtained from repeated solution of the microscopic problem (3), i.e., evaluation of Φ over N strain paths, as the surrogate for Φ. In this approach, there is no empirical model as in the classical setting, or any architecture as in the machine-learnt setting of Section 4. The method was initially developed where D was experimental data, but can be applied to the multiscale setting as we describe presently.

The computational sciences, as applied to physics and engineering problems, have always been about using data inputs to predict outcomes. Computational science differs from generic data science (cf., e. g., Agarwal et al., 2016; Agarwal and Dhar, 2014; Agarwal et al., 2011; Baesens, 2014) in that the problems of interest are constrained by physical laws. Such physical laws find mathematical expression in the form of field equations such as conservation of linear momentum in mechanics, conservation of mass in transport problems, Maxwell's equations in electromagnetism, and others. Many of the methodologies that have been developed since the dawn of modern numerical analysis in the 1950's have been preoccupied with discretizing those exactly-known field equations. Finite differences, finite elements, finite volumes, molecular dynamics and mesh-free methods are all examples of different ways of approximating field equations.

By contrast, material laws have traditionally been uncertain and imperfectly known owing to the paucity of observational data, experimental error or intrinsic stochasticity of the material behavior. A common response to this imperfect knowledge has been modeling. Models are designed to act as succinct summaries of complex material data for which summarization is a difficult task. They are also used to characterize material behavior across regimes that are data sparse. To that end, material modeling relies on heuristics and intuition, which inevitably results in loss of information, biasing, modeling error and epistemic uncertainty. Adding to these difficulties, material modeling is open-ended, i. e., there is no theory that dictates how sequences of models of increasing accuracy and fidelity can be generated that are sure to converge to the actual – and unknown – material law.

For instance, a common approach to material modeling is to assume a relation of the form

$$\sigma = g(\epsilon) + \eta, \tag{8}$$

where ϵ and σ are local work-conjugate variables characteristic of the material, g is a deterministic material law and η represents observational noise. In practice, the essential difficulty is that neither g nor the distribution of η are known. General principles do not suffice to

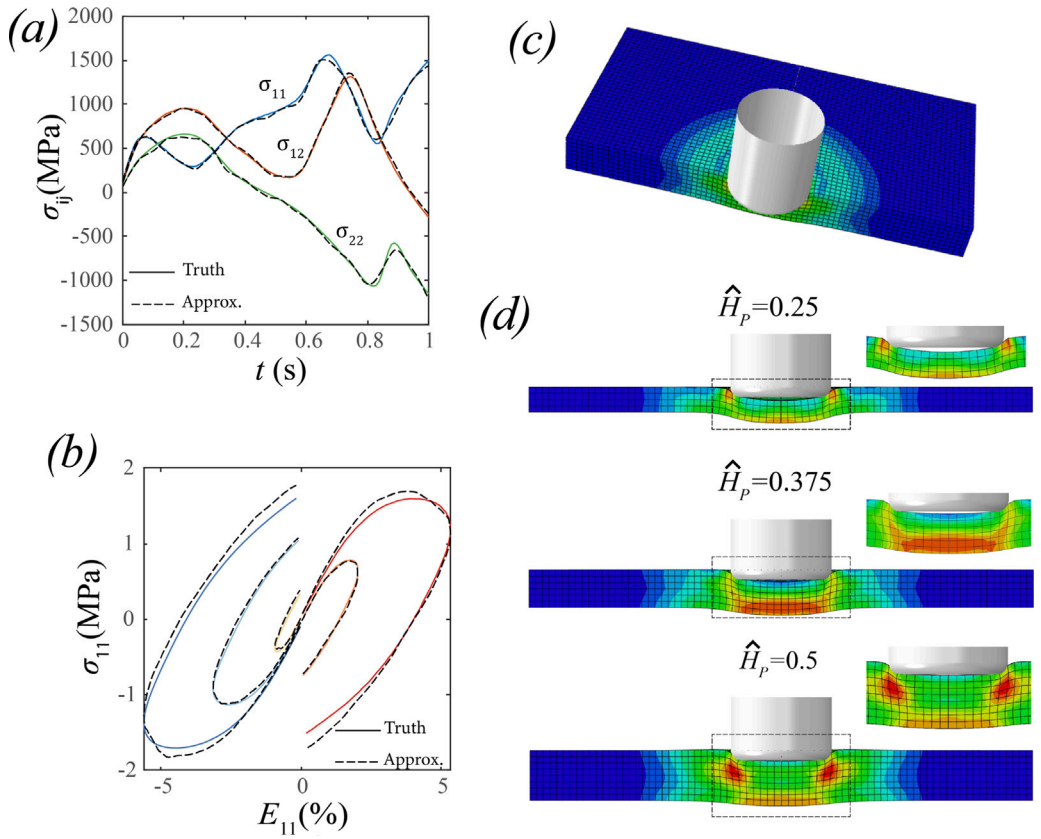

Fig. 8. Demonstration on impact of a polycrystalline material plate. (a, b) Predictive ability of machine-learned surrogate for deformation of polycrystalline Mg. (c) Ballistic plate impact and (d) design study of plate thickness using machine-learned surrogate.

determine g uniquely with material specificity and considerable latitude is left to the modeler as regards material identification. A common approach is to determine g by recursion and fitting to empirical data, e. g., by means of machine learning. Here again, considerable latitude is left to the modeler as regards the type of functions and criteria to be used for purposes of recursion and representation. For stochastic systems, the situation is greatly compounded by the fact that the prior probability distribution from which the noise η is drawn is generally not known and needs to be modeled as well.

Against this backdrop, the staggering developments in experimental science and microscopy, which produce large sets of fully-resolved 3D material data, constitute a veritable game changer. By virtue of those advances, scientific computing has transitioned from being data-poor to being data-rich. This sea change raises the question of whether a more direct connection between material data and prediction can be effected, specifically one where the intervening modeling step is eliminated altogether. A notional comparison between classical and model-free inference is

Classical inference:
Data → Model → Prediction
Model-Free Data-Driven inference:
Data ⟶ Prediction

Here, modeling is understood as any operation that modifies the data set or replaces it by another object, be it through constitutive modeling, fitting, model reduction, regression, machine learning, or any other operation. By model-free we understand methods of inference that use the data, all the data and nothing but the data for purposes of prediction. Material behavior is explicitly defined by the source data associations and modeling empiricism, error and uncertainty are eliminated entirely.

There is considerable ongoing work aimed at developing this emerging Model-Free Data-Driven paradigm. The initial proposal (Kirchdoerfer and Ortiz, 2016) developed a distance-minimizing approach that converges for sequences of uniformly convergent data sets. Subsequent work (Kirchdoerfer and Ortiz, 2017) made use of a max-ent information theory in order to render the approach robust with respect to noise and outliers in the data set. The distance minimization approach has also been extended to infinite-dimensional boundary-value problems, including linear and finite elasticity (Conti et al., 2018, 2020; Platzer et al., 2021). This extension differs fundamentally from the finite-dimensional setting in that relaxation, or the emergence of weakly convergence fine spatial oscillations that exploit the structure of the data set, plays an essential role. Remarkably, relaxation sets forth a notion of convergence with respect to data, or Δ-convergence that is fundamentally different from the classical relaxation of energy functionals. Extensions of Model-Free Data-Driven analysis to dynamics and inelastic materials require consideration of evolving data sets conditioned by the prior history of the material (Kirchdoerfer and Ortiz, 2018; Eggersmann et al., 2019; Carrara et al., 2020).

The Model-Free Data-Driven paradigm also sets forth a novel alternative to calculus of variations, concurrent and parameter-passing schemes in multiscale modeling. Specifically, one can use offline microscale calculations in order to generate material data sets for Model-Free Data-Driven computing at the macroscale. This is a fully automated approach that requires no modeling or analysis at the macroscale and requires no fitting of the micromechanical data. The approach is lossless in that it uses the generated micromechanical data, all the data and nothing but the data.

Karapiperis et al. (2021) have demonstrated the approach by means of an application to granular media. Specifically, they rely on the Level-Set Discrete Element Method (LS-DEM) (Kawamoto et al., 2016) to generate material data sets for angular (Hostun) sand, Fig. 9. The virtual specimen is deformed along selected loading and unloading paths

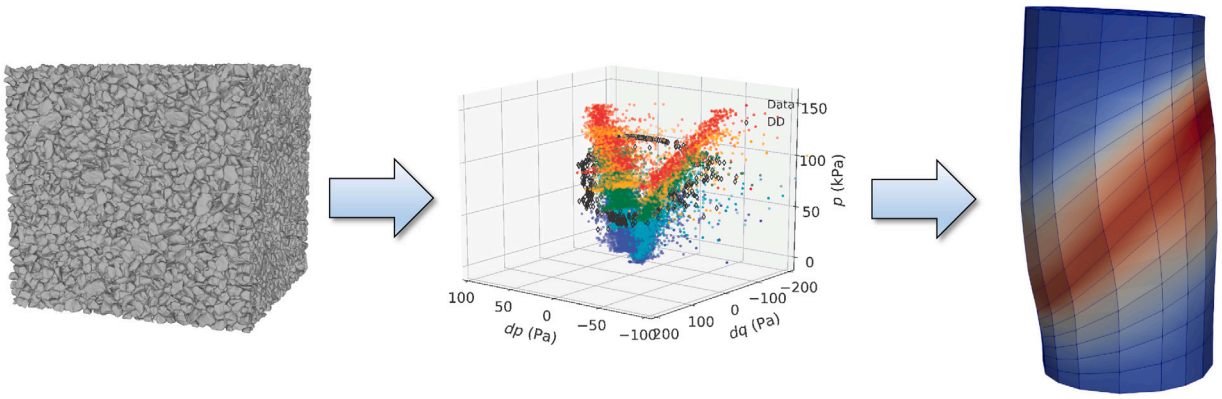

Fig. 9. Model-Free Data-Driven multiscale analysis of plane-strain uniaxial compression test of Karapiperis et al. (2021). Left: Representative volume element for micromechanical calculations. Middle: Sample data computed by deforming RVE along selected strain paths using the Level-Set Discrete Element Method (LS-DEM) (Kawamoto et al., 2016). Right: Model-Free Data-Driven finite-element calculation of a triaxial compression experiment on a specimen of angular (Hostun) sand (Andò et al., 2012) built on the RVE data.

to produce material data sets including stress, strain, internal energy and dissipation, in accordance with an energy-based parametrization of the data. A representative data set is shown in Fig. 9. The data thus obtained can be used, *in toto*, as a basis for Model-Free Data-Driven calculations at the macroscale. Fig. 9 depicts one such simulation of an *in-situ* triaxial compression experiment on a specimen of angular (Hostun) sand (Andò et al., 2012). The specimen is first compressed isotropically to 100 kPa, and then compressed triaxially by keeping the cell pressure constant while prescribing a vertical displacement to the platen under quasistatic conditions. Failure is computed to occur through the formation of a persistent shear band, which agrees well with experimental observations (Andò et al., 2012). The axial strains, principal stress ratio and volumetric strains predicted by the Model-Free Data-Driven simulation are also in good agreement with experimental measurements.

It bears emphasis that, in this approach, the micromechanical data is lifted into the macromechanical calculations losslessly and without modification, i. e., without modeling of any type. This direct link between data and prediction effectively cuts through the Gordian knot of multiscale upscaling and the representation of the effective macroscopic behavior.

Data-Driven methods are likely to gain importance at a time when data from high-fidelity simulations and high-resolution experiments are becoming increasingly abundant. The Model-Free Data-Driven paradigm, in particular, possesses ancillary attributes that add to its appeal. Thus, it standardizes solvers by separating the treatment of the field equations from the characterization of material behavior. Specifically, Model-Free Data-Driven computing reduces boundary value problems to the solution of two standard *linear* problems, regardless of material behavior. The interaction between the solver and the material data repository reduces to data searches and data transfer that can also be standardized and scripted non-intrusively. In particular, the data repositories can be centralized, developed and maintained remotely from the locally run solver software. This data and work-flow structure allow material data sets of disparate provenances to be pooled together and has the potential for changing the way in which material data is developed, stored, exchanged and disseminated in science and in industry.

6. Uncertainty quantification across scales

A key aspect of the materials-by-design approach is the recognition that properties of real materials are the result of complex multiscale phenomena. The complexity of the material behavior across scales is the main source of uncertainty in engineering applications. Consider the two-scale setting described in Section 2. We have uncertainties in the microscopic material parameter P, uncertainties in the texture or microstructure, uncertainties due to the introduction of the surrogate, and uncertainties in the configuration. All of these affect the overall performance, and we seek to quantify the uncertainty in the overall performance due to uncertainties in the various inputs and surrogates.

Unfortunately, the direct estimation of integral or system level uncertainties requires repeated evaluations of entire system aimed at determining worst-case scenarios at all scales resulting in the largest deviations in macroscopic behavior. Such integral calculations are prohibitively expensive in terms of computational cost and are beyond the scope of the present-day computers.

We describe a framework to quantify the propagation of uncertainties through length scales (Sun et al., 2020; Liu et al., 2021) in an efficient manner. It is based on the observation that the multiscale modeling may be described as a nested composition of maps. For example, the map from the inputs (microscopic material parameter P, texture T, microscopic material models $\{W, D\}$, surrogate $\tilde{\Phi}$, configuration C) to the output (objective O) in Fig. 3 has the structure

$$O = M(\tilde{\Phi}(\Phi(P, T, W, D), s), C) \tag{9}$$

where s represents the choice of the surrogate, and M is the macroscopic model. Alternately, the map may be represented as a directed graph as shown in Fig. 10, left. The key idea is that one can explore this nested or direct graph structure to compute the individual uncertainties and then compose them. We can do so rigorously when we seek rigorous upper bounds on the integral uncertainties. McDiarmid's inequality (McDiarmid, 1989) provides rigorous upper bounds on the uncertainty of the output of a function in terms of the uncertainties of the inputs. The key characteristic that determines this uncertainty is the so-called modulus of continuity. Importantly the bounds become sharper with an increasing number of input variables which is known as the concentration-of-measure phenomenon (Ledoux, 2001). Now, it is possible to bound the overall or integral or system-level modulus of uncertainty of a nested map in the terms of the moduli of continuity of the individual maps (Topcu et al., 2011). Therefore, we can evaluate the rigorous upper bound of the system-level uncertainty in terms of the uncertainties at each subsystem. Thus, no integral or system-level calculation is required, and the evaluation of uncertainty of the multi-scale system becomes computationally feasible.

The approach has been used to assess the ballistic impact of magnesium plate, as depicted in Fig. 10. The material model $\{W, D\}$ includes slip and twinning at the single crystal level, the microscopic model Φ is the polycrystalline response that is computed using Taylor averaging, the surrogate $\tilde{\Phi}$ is a Johnson–Cook constitutive model and macroscopic model M is the ballistic performance of the magnesium plate is simulated using finite elements. We then study the uncertainty of the ballistic response due to uncertainties in the strength of

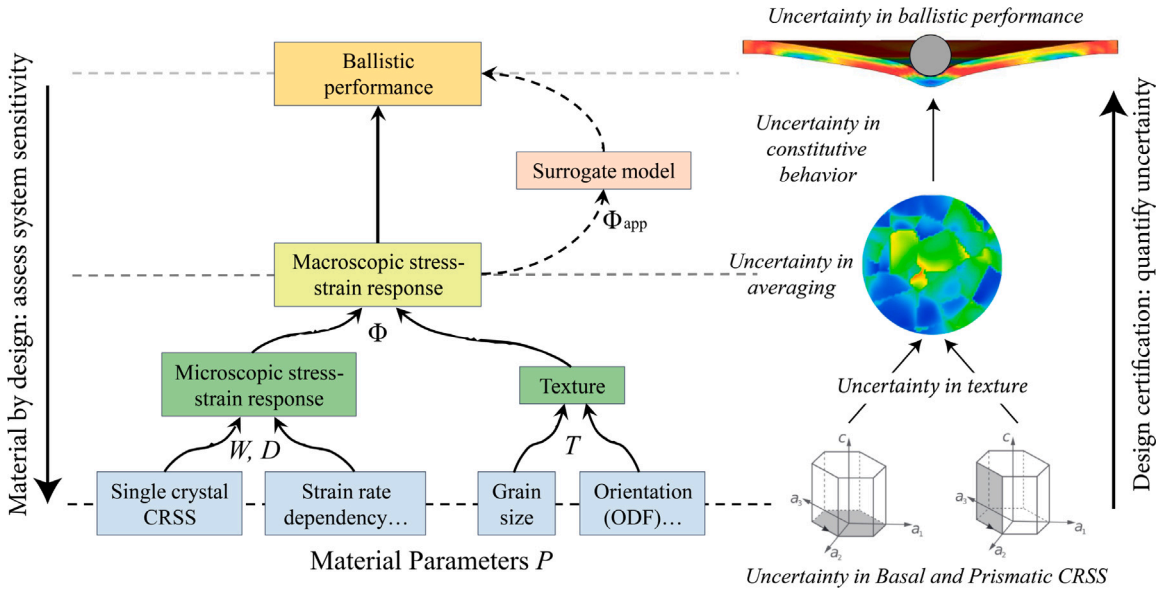

Fig. 10. Hierarchical multiscale uncertainty quantification of magnesium.

(a)

Basal $\langle a \rangle$	Prismatic $\langle a \rangle$	Pyramidal $\langle c+a \rangle$	Tensile twin
[0.44 4.16]	[17.0 50.0]	[27.76 86.0]	[1.86 11.7]

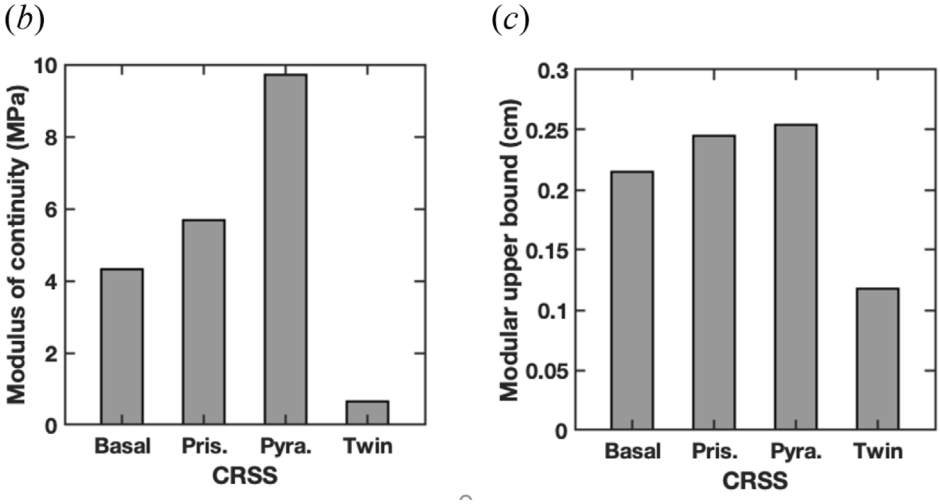

Fig. 11. Multiscale uncertainty of Magnesium plate. (a) Uncertainties in slip and twin critical resolved shear stress (CRSS). Unit: MPa. (b) Micro to meso uncertainty quantification showing the variation in Johnson Cook parameter from different CRSS. (c) Micro to macro uncertainty quantification showing the variation in backface deflection (modular upper bound) from different CRSS.

individual slip and twin systems. In particular, we assume all the micro-scale parameters are uncertainty free except the slip and twin critical resolved shear stress (CRSS) (Liu et al., 2021), see Fig. 11(a). The micro-scale uncertainty results in the uncertainties of the meso-scale Johnson Cook parameters and eventually the macroscale back-face deflection (quantity of interest).

The resultant micro to meso uncertainty propagation and micro to macro uncertainty propagation are demonstrated in Fig. 11(b) and (c) respectively. An important property of the moduli of continuity is that, since they are dimensionally homogeneous, they can be compared and rank-ordered, which in turn provides a quantitative metric of the relative contributions of the input parameters to the overall uncertainty. The rank-ordering of the CRSSs to the overall uncertainty in ballistic performance is found to be pyramidal>prismatic>basal>twin, with the pyramidal and prismatic CRSSs contributing the most, the twin CRSS the least and the basal CRSS in between. The calculations show that the integral uncertainties determined by the hierarchical multiscale UQ approach are sufficiently tight for use in engineering applications. The analysis also sheds light on the relative contributions of the different unit mechanisms (i.e., slip and twin systems) to the integral uncertainty and the dominant propagation paths for uncertainty across the model hierarchy.

It bears emphasis that the computational expense of the hierarchical UQ framework can be much smaller compared with integral calculations, especially when lower scale calculations tend to be extremely expensive. The analysis in Ref. Liu et al. (2021) shows that the difference of computational cost scales exponentially with the number of levels in the hierarchy. Moreover, the proposed approach is rigorous,

and provides a bound. An obvious limitation is the possibility that this bound is too conservative to be useful. The current example shows that it is not so on this occasion. Further, increasing tightness comes at increasing extent of data through either experimental or lower-level computational tests. Simple information of parameter bounds used in the present work supplies a working compromise between tightness and expense. However, it is both interesting and useful to investigate the tightness of the bounds and the attendant conservativeness of the designs by increasing additional information of random inputs. For instance, when the bounds on the moments of random inputs are known, the optimal uncertainty quantification (OUQ) protocol (Owhadi et al., 2013; Kamga et al., 2014) is capable of taking into account all such information about input distributions by reduction theorem and then providing optimal bounds on the probability of failure by leveraging all the known information.

Finally, we remark on the comparison between the proposed approach and Bayesian strategies. Bayesian inference, based on the Bayes' theorem, has been introduced as one of the main tools for UQ of the computational models (Honarmandi and Arróyave, 2020), mainly due to the relative simplicity of implementation and the rigor of the resulting Bayesian analysis. Nevertheless, the quantification of uncertainties is conducted via calculating high-dimensional integrals that are very intractable or even impossible to evaluate analytically through conventional integration techniques (Lynch, 2007), let alone those significantly complicated response functions that are achieved by existing open-source codes or commercial software. One numerical way to solve those integrals is Monte-Carlo sampling (Lucas et al., 2008), which can become impractical if the probability of failure is small, i.e., if failure is a rare event, and if one-call of forward calculation is costly. By way of contrast, in the proposed method the response function at each length-scale of the hierarchical structure can effectively be treated as a black-box and the effort required for the computation of the uncertainty bounds is independent of the size of the probability of failure. In addition, the most commonly used priors in engineering problems are uniform and normal distributions. However, the strong influence of priors on the outcome of the inference process is also one of the most significant criticisms of Bayesian frameworks (Wolpert, 1996). By contrast, our approach only requires the intervals of uncertain parameters and then provides rigorous bounds on the output uncertainties that bracket all the possible results led by all the probability measures in such intervals.

7. Concurrent optimization of material and structure

The performance of modern devices typically depends on the properties of their component materials that operate across a broad range of disparate time- and length-scales (Sun et al., 2017, 2019; Zheng et al., 2016). Due to recent advancements in nanotechnology, materials characterization and synthesis, additive manufacturing, and high-performance computing, it is possible to develop innovative advanced materials with sophisticated structures and multiple properties from the atomistic to the macroscopic application scale (Sun et al., 2018; Pikul et al., 2019; Meza et al., 2014). For instance, mechanical properties can be tailored by adjusting microstructures, material constitutions, their spatial distribution and mass fractions using material synthesis and processing (Yogeshvaran et al., 2020; Bhattacharya, 2003; Liu et al., 2019a). On the other hand, structural properties, e. g., size and shape of components, can be controlled by material manufacturing such as 3D printing at different length-scales (Wong and Hernandez, 2012; Schaedler et al., 2011; Schumacher et al., 2015).

Traditionally, a device can be designed in a *sequential* manner. First, each individual component material is optimized over its desired design properties separately in very simple tests, or even by *serendipitous* discoveries. Then, the device, as a whole system, is designed with respect to the rest of the properties, e. g., the distribution and fraction of component materials in the device, whereas the properties of each component are fixed at the "optimal" results determined from the previous step. However, there exist two critical challenges in this sequential optimization process. First, the attainment of all the best properties is a vital requirement for most materials; unfortunately these properties are generally mutually exclusive, e. g., the conflict between strength and toughness. Therefore, how to account for the correlations between design properties of component materials poses a significant challenge to the development of new devices in the applications of interest. Second, the sequential process neglects the connection between component materials, and the connection between the entire device and its application environments. As a result, the performance of the device might be underestimated over the accessible ranges of its design properties.

In the context of Section 2, we seek to optimize the objective O over material properties P and the configuration. In the traditional sequential approach, we first optimize some effective material behavior (related to Φ) and with this optimal material held fixed, we optimize O over the configuration. However, this may lead to a sub-optimal solution when we optimize O over both configuration and material.

In order to address the aforementioned problems, we have proposed a *joint* design strategy (Sun et al., 2021). We do so in a single scale model where the material parameters describe the macroscopic model. The basic idea behind this strategy is that, the device with its components is regarded as a whole system and the design process is directly related to the application where the device operates. To this end, the design variables include both the properties of each individual component material and the properties connecting the components with the device. The design objective is to maximize a crucial metric that characterizes the targeted performance of the device in the application. At the same time, the correlations between material properties are taken into account by employing ellipsoid convex sets as inequality constraints in the optimization (Jiang et al., 2011, 2013), as illustrated in Fig. 12(a). As a result, the design of the device is formulated as a constrained co-optimization problem that is solved over all the design parameters *simultaneously*. We specifically consider the mechanical and structural design variables of the device and have developed a non-intrusive, high-performance computational framework, Fig. 12(b), based on DAKOTA Version 6.12 software package (Adams et al., 2020) of the Sandia National Laboratories. We have also implemented Gmsh Version 4.5.4 software package (Geuzaine and Remacle, 2009) in the framework, since the optimization requires evaluation of different structural parameters and therefore may need to generate meshes for the device on-the-fly.

We assess the sequential and joint design strategies in an application where the ballistic performance of a double-layered plate is optimized using alternating AZ31B magnesium alloy and polyurea, as depicted in Fig. 13. Schematic illustrations of the two design strategies in this application are shown in Figs. 13(a)–(d). Specifically, we consider a scenario in which normal impact and full perforation take place during the impact process. The design objective is assumed to be a minimum residual velocity v_r of the projectile after penetrating the plate. The design variables include the mechanical properties of AZ31B and polyurea that govern the strength and toughness of materials, and the structural parameters of component layers, i. e., their thicknesses. The constraints include a fixed total mass of the plate M_{tot} and ellipsoid convex sets on the mechanical properties of AZ31B and polyurea. Fig. 13(e) compares the residual velocity at the optimal mechanical and structural parameters using different values of M_{tot}. Notably, using residual velocity as a reference, the proposed joint design strategy can greatly improve the performance at the intermediate values of the plate mass compared to the traditional sequential design approach. Importantly, our result not only agrees well with the classical knowledge in ballistic protection systems that a combination of strong and stiff front layer with a soft but tough back layer provides the optimal ballistic performance (O'Masta et al., 2014; Liu et al., 2019c,b), but also provides a quantitative optimal solution of the design. Therefore, the proposed method has provided new insights for designing novel materials with significant desired application performance.

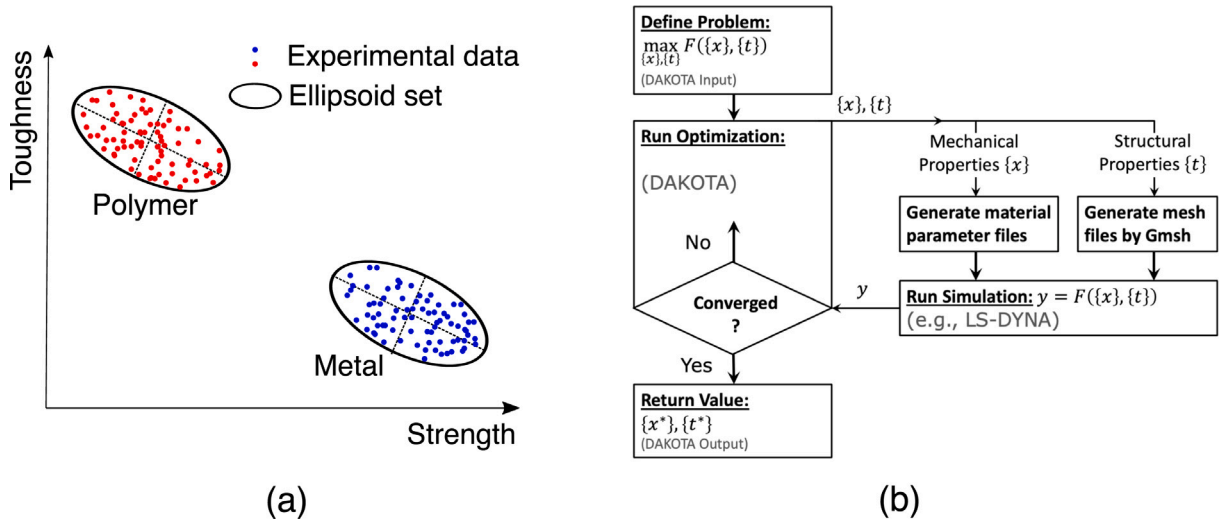

Fig. 12. (a) Schematic illustration of conflict between mechanical properties. (b) Flowchart of joint design strategy over mechanical and structural properties.

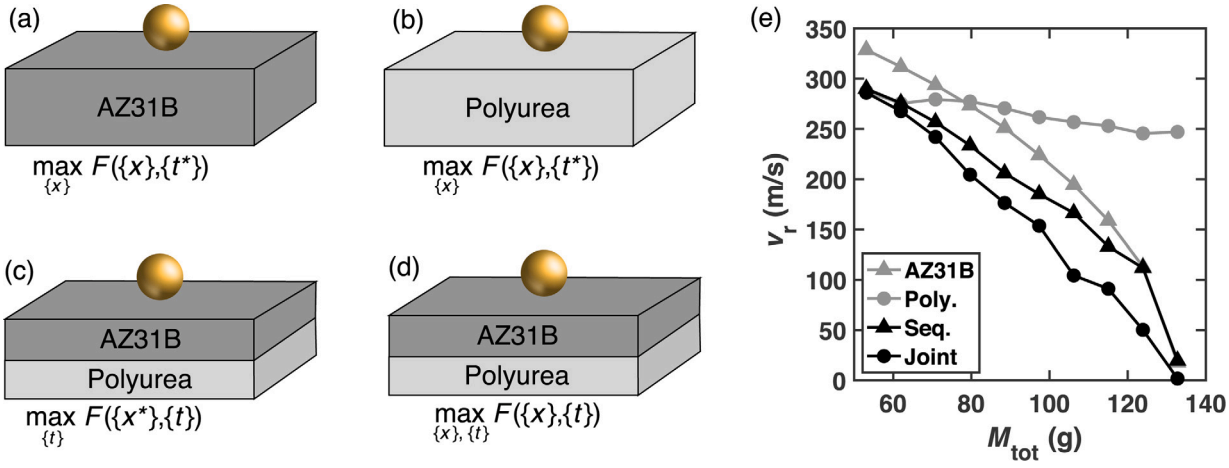

Fig. 13. Strategies and results of designing a multi-layered plate subject to high-speed impact. (a) Design over mechanical properties of AZ31B. (b) Design over mechanical properties of polyurea. (c) Design over structural properties of layers. Steps (a), (b) and (c) form the strategy of sequential design. (d) Joint design over mechanical and structural properties. (e) Comparison of residual velocity at different values of plate mass.

8. Summary

In this paper, we have reviewed a number of recent developments in methodology that advance the goal of designing materials targeted by specific applications. The macroscopic behavior of materials is the end result of a number of mechanisms that operate across a broad range of disparate scales. Multiscale modeling seeks to address this complexity using a 'divide and conquer' approach where range of material behavior is first divided into an ordered hierarchy of scales. Section 3 describes how emerging computational platforms that use accelerators like GPUs can be effectively used to study problems at individual scales. The scales are then linked using an approach where the higher scale model modulates the lower scale behavior, but also averages its outcome. Section 4 shows how machine learning can be effectively used for this scale transition. Section 5 describes an entirely new approach of model-free simulations where the data – experimental or computational from lower scale models – can be exploited directly. The complexity of multiscale modeling also introduces uncertainty at various scales. Section 6 shows how we can exploit the hierarchical nature of multiscale modeling to quantify integral uncertainties by studying individual uncertainties. Finally, we explore the joint optimization of material and structure in Section 7.

Declaration of competing interest

The authors declare that they have no known competing financial interests or personal relationships that could have appeared to influence the work reported in this paper.

Acknowledgments

The work described in Sections 4, 6 and 7 was sponsored by the Army Research Laboratory, United States and was accomplished under Cooperative Agreement Number W911NF-12-2-0022. The views and conclusions contained in this document are those of the authors and should not be interpreted as representing the official policies, either expressed or implied, of the Army Research Laboratory or the U.S. Government. The U.S. Government is authorized to reproduce and distribute reprints for Government purposes notwithstanding any copyright notation herein The work described in Section 3 was sponsored by the Air Force Office of Scientific Research, United States under the MURI Award FA9550-16-1-0566. The work described in Section 5 was sponsored by the Air Force Office of Scientific Research, United States through the Center of Excellence on High-Rate Deformation Physics of Heterogeneous Materials, Award FA9550-12-1-0091 and the Deutsche Forschungsgemeinschaft, Germany through the Sonderforschungsbereich 1060 'The mathematics of emergent effects'.

References

Adams, B.M., Bohnhoff, W.J., Dalbey, K.R., Ebeida, M.S., Eddy, J.P., Eldred, M.S., Hooper, R.W., Hough, P.D., Hu, K.T., Jakeman, J.D., Khalil, M., Maupin, K.A., Monschke, J.A., Ridgway, E.M., Rushdi, A.A., Seidl, D.T., Stephens, J.A., Swiler, L.P., Winokur, J.G., 2020. Dakota, a multilevel parallel object-oriented framework for design optimization, parameter estimation, uncertainty quantification, and sensitivity analysis: version 6.12 user's manual. Tech. Rep., Sandia National Laboratories, pp. 2020–5001, SAND.

Agarwal, D., Cheah, Y.W., Fay, D., Fay, J., Guo, D., Hey, T., Humphrey, M., Jackson, K., Li, J., Poulain, C., Ryu, Y., van Ingen, C., 2011. Data-intensive science: The terapixel and modisazure projects. Int. J. High Perform. Comput. Appl. 25 (3), 304–316.

Agarwal, R., Dhar, V., 2014. Big data, data science, and analytics: The opportunity and challenge for IS research. Inf. Syst. Res. 25 (3), 443–448.

Agarwal, D.A., Faybishenko, B., Freedman, V.L., Krishnan, H., Kushner, G., Lansing, C., Porter, E., Romosan, A., Shoshani, A., Wainwright, H., Weidmer, A., Wu, K.S., 2016. A science data gateway for environmental management. Concurr. Computation-Practice Exp. 28 (7), 1994–2004.

Andò, E., Hall, S., Viggiani, G., Desrues, J., Bésuelle, P., 2012. Grain-scale experimental investigation of localised deformation in sand: a discrete particle tracking approach. Acta Geotech. 7 (1), 1–13.

Anglin, B., Lebensohn, R., Rollett, A., 2014. Validation of a numerical method based on fast Fourier transforms for heterogeneous thermoelastic materials by comparison with analytical solutions. Comput. Mater. Sci. 87, 209–217.

Baesens, B., 2014. Analytics in a Big Data World : The Essential Guide to Data Science and its Applications. In: Wiley & SAS business series, xv, John Wiley & Sons, Inc., Hoboken, New Jersey, p. 232.

Balasubramanian, S., Anand, L., 2002. Elasto-viscoplastic constitutive equations for polycrystalline fcc materials at low homologous temperatures. J. Mech. Phys. Solids 50, 101–126.

Bensoussan, A., Lions, J.-L., Papanicolaou, G., 2011. Asymptotic Analysis for Periodic Structures. vol. 374, American Mathematical Soc..

Berbenni, S., Taupin, V., Lebensohn, R.A., 2020. A fast Fourier transform-based mesoscale field dislocation mechanics study of grain size effects and reversible plasticity in polycrystals. J. Mech. Phys. Solids 135, 103808.

Bertin, N., Capolungo, L., 2018. A FFT-based formulation for discrete dislocation dynamics in heterogeneous media. J. Comput. Phys. 355, 366–384.

Bhattacharya, K., 2003. Microstructure of Martensite: Why It Forms and how It Gives Rise To the Shape-Memory Effect. Oxford University Press.

Bhattacharya, K., Hosseini, B., Kovachki, N.B., Stuart, A.M., 2021. Model reduction and neural networks for parametric pdes. SMAI J. Comput. Math. 7, 121–157.

Bhattacharya, K., Suquet, P., 2005. A model problem concerning recoverable strains of shape-memory polycrystals. Proc. R. Soc. Lond. Ser. A Math. Phys. Eng. Sci. 461, 2797–2816.

de Borst, R., Ramm, E., 2011. Multiscale Methods in Computational Mechanics. Springer, Heidelberg.

Boyd, S., Parikh, N., Chu, E., Peleato, B., Eckstein, J., et al., 2011. Distributed optimization and statistical learning via the alternating direction method of multipliers. Found. Trends Mach. Learn. 3, 1–122.

Carrara, P., De Lorenzis, L., Stainier, L., Ortiz, M., 2020. Data-driven fracture mechanics. Comput. Methods Appl. Mech. Engrg. 372, 113390.

Chen, Z., Daly, S., 2018. Deformation twin identification in magnesium through clustering and computer vision. Mater. Sci. Eng. A 736, 61–75.

Cheng, T., Jaramillo-Botero, A., An, Q., Ilyin, D.V., Naserifar, S., Goddard, W.A., 2019. First principles-based multiscale atomistic methods for input into first principles nonequilibrium transport across interfaces. Proc. Natl. Acad. Sci. 116, 18193–18201.

Cole, D.J., Mones, L., Csányi, G., 2020. A machine learning based intramolecular potential for a flexible organic molecule. Faraday Discuss. 224, 247–264.

Collobert, R., Weston, J., 2008. A unified architecture for natural language processing: Deep neural networks with multitask learning. In: Proceedings of the 25th International Conference on Machine Learning. pp. 160–167.

Conti, S., Müller, S., Ortiz, M., 2018. Data-driven problems in elasticity. Arch. Ration. Mech. Anal. 229 (1), 79–123.

Conti, S., Müller, S., Ortiz, M., 2020. Data-driven finite elasticity. Arch. Ration. Mech. Anal. 237 (1), 133.

De Graef, M., 2020. A dictionary indexing approach for EBSD. Mater. Sci. Eng. 891, 012009.

Eggersmann, R., Kirchdoerfer, T., Reese, S., Stainier, L., Ortiz, M., 2019. Model-free data-driven inelasticity. Comput. Methods Appl. Mech. Engrg. 350, 81–99.

Eghtesad, A., Zecevic, M., Lebensohn, R.A., McCabe, R.J., Knezevic, M., 2018. Spectral database constitutive representation within a spectral micromechanical solver for computationally efficient polycrystal plasticity modelling. Comput. Mech. 61, 89–104.

Feyel, F., Chaboche, J.-L., 2000. FE2 multiscale approach for modelling the elasto-viscoplastic behaviour of long fibre SiC/Ti composite materials. Comput. Methods Appl. Mech. Engrg. 183, 309–330.

Fish, E., 2009. Multiscale Methods: Bridging the Scales in Science and Engineering. Oxford University Press, Oxford.

Fu, C.-C., Dalla Torre, J., Willaime, F., Bocquet, J.-L., Barbu, A., 2005. Multiscale modelling of defect kinetics in irradiated iron. Nature Mater. 4, 68–74.

Geuzaine, C., Remacle, J.-F., 2009. Gmsh: A 3-D finite element mesh generator with built-in pre-and post-processing facilities. Internat. J. Numer. Methods Engrg. 79 (11), 1309–1331.

Glowinski, R., 2015. Variational Methods for the Numerical Solution of Nonlinear Elliptic Problems. Society for Industrial and Applied Mathematics, Philadelphia, PA.

Goldberg, Y., 2017. Neural network methods for natural language processing. Synth. Lect. Hum. Lang. Technol. 10, 1–309.

He, K., Zhang, X., Ren, S., Sun, J., 2016. Deep residual learning for image recognition. In: Proceedings of the IEEE Conference on Computer Vision and Pattern Recognition. pp. 770–778.

Honarmandi, P., Arróyave, R., 2020. Uncertainty quantification and propagation in computational materials science and simulation-assisted materials design. Integr. Mater. Manuf. Innov. 9 (1), 103–143.

Jain, A., Ong, S.P., Hautier, G., Chen, W., Richards, W.D., Dacek, S., Cholia, S., Gunter, D., Skinner, D., Ceder, G., 2013. The materials project: A materials genome approach to accelerating materials innovation. APL Mater. 1, 011002.

Jiang, C., Bi, R., Lu, G., Han, X., 2013. Structural reliability analysis using non-probabilistic convex model. Comput. Methods Appl. Mech. Engrg. 254, 83–98.

Jiang, C., Han, X., Lu, G., Liu, J., Zhang, Z., Bai, Y., 2011. Correlation analysis of non-probabilistic convex model and corresponding structural reliability technique. Comput. Methods Appl. Mech. Engrg. 200 (33–36), 2528–2546.

Jordan, B., Gorji, M.B., Mohr, D., 2020. Neural network model describing the temperature-and rate-dependent stress-strain response of polypropylene. Int. J. Plast. 135, 102811.

Kalidindi, S., De Graef, M., 2015. Materials data science: current status and future outlook. Annu. Rev. Mater. Res. 45, 171–193.

Kamga, P.-H., Li, B., McKerns, M., Nguyen, L., Ortiz, M., Owhadi, H., Sullivan, T., 2014. Optimal uncertainty quantification with model uncertainty and legacy data. J. Mech. Phys. Solids 72, 1–19.

Karapiperis, K., Stainier, L., Ortiz, M., Andrade, J., 2021. Data-driven multiscale modeling in mechanics. J. Mech. Phys. Solids 147, 104239.

Kawamoto, R., Andó, E., Viggiani, G., Andrade, J.E., 2016. Level set discrete element method for three-dimensional computations with triaxial case study. J. Mech. Phys. Solids 91, 1–13.

Kirchdoerfer, T., Ortiz, M., 2016. Data-driven computational mechanics. Comput. Methods Appl. Mech. Engrg. 304, 81–101.

Kirchdoerfer, T., Ortiz, M., 2017. Data driven computing with noisy material data sets. Comput. Methods Appl. Mech. Engrg..

Kirchdoerfer, T., Ortiz, M., 2018. Data-driven computing in dynamics. Internat. J. Numer. Methods Engrg. 113 (11), 1697–1710.

Kirk, D.B., Hwu, W.-M.W., 2016. Programming Massively Parallel Processors. Morgan-Kaufman.

Knezevic, M., Savage, D.J., 2014. A high-performance computational framework for fast crystal plasticity simulations. Comput. Mater. Sci. 83, 101–106.

Kothe, D., Lee, S., Qualters, I., 2019. Exascale computing in the United States. Comput. Sci. Eng. 21, 17–29.

Le, B., Yvonnet, J., He, Q.-C., 2015. Computational homogenization of nonlinear elastic materials using neural networks. Internat. J. Numer. Methods Engrg. 104 (12), 1061–1084.

Lebensohn, R.A., Needleman, A., 2016. Numerical implementation of non-local polycrystal plasticity using fast Fourier transforms. J. Mech. Phys. Solids 97, 333–351.

LeCun, Y., Bengio, Y., et al., 1995. Convolutional networks for images, speech, and time series. Handb. Brain Theory Neural Netw. 3361 (10), 1995.

Ledoux, M., 2001. The Concentration of Measure Phenomenon. American Mathematical Soc..

Li, Z., Kovachki, N., Azizzadenesheli, K., Liu, B., Bhattacharya, K., Stuart, A., Anandkumar, A., 2020. Multipole graph neural operator for parametric partial differential equations. Adv. Neural Inf. Process. Syst. 33, 1–17.

Li, Z., Kovachki, N., Azizzadenesheli, K., Liu, B., Bhattacharya, K., Stuart, A., Anandkumar, A., 2021. Fourier Neural operator for parametric partial differential equations. In: International Conference on Learning Representations. pp. 1–16.

Liu, B., Kandan, K., Wadley, H., Deshpande, V., 2019a. Deep penetration of ultra-high molecular weight polyethylene composites by a sharp-tipped punch. J. Mech. Phys. Solids 123, 80–102.

Liu, B., Kandan, K., Wadley, H., Deshpande, V., 2019b. High strain rate compressive response of ultra-high molecular weight polyethylene fibre composites. Int. J. Plast. 122, 115–134.

Liu, B., Kovachki, N., Li, Z., Azizzadenesheli, K., Anandkumar, A., Stuart, A., Bhattacharya, K., 2022. A learning-based multiscale method and its application to inelastic impact problems . J. Mech. Phys. Solids 158, 104668.

Liu, B., Sun, X., Bhattacharya, K., Ortiz, M., 2021. Hierarchical multiscale quantification of material uncertainty. J. Mech. Phys. Solids 153, 104492.

Liu, B., Wadley, H., Deshpande, V., 2019c. Failure mechanism maps for ultra-high molecular weight polyethylene fibre composite beams impacted by blunt projectiles. Int. J. Solids Struct. 178, 180–198.

Liu, Z., Wu, C., Koishi, M., 2019d. A deep material network for multiscale topology learning and accelerated nonlinear modeling of heterogeneous materials. Comput. Methods Appl. Mech. Engrg. 345, 1138–1168.
Lucas, L.J., Owhadi, H., Ortiz, M., 2008. Rigorous verification, validation, uncertainty quantification and certification through concentration-of-measure inequalities. Comput. Methods Appl. Mech. Engrg. 197 (51–52), 4591–4609.
Ludwig, A., 2019. Discovery of new materials using combinatorial synthesis and high-throughput characterization of thin-film materials libraries combined with computational methods. Npj Comput. Mater. 5, 70.
Lynch, S.M., 2007. Introduction To Applied Bayesian Statistics and Estimation for Social Scientists. Springer Science & Business Media.
Marchand, D., Jain, A., Glensk, A., Curtin, W., 2020. Machine learning for metallurgy I. A neural-network potential for Al-Cu. Phys. Rev. Mater. 4 (10), 103601.
McCormick, N., Lord, J., 2010. Digital image correlation. Mater. Today 13 (12), 52–54.
McDiarmid, C., 1989. On the method of bounded differences. Surv. Combin. 141 (1), 148–188.
Meza, L.R., Das, S., Greer, J.R., 2014. Strong, lightweight, and recoverable three-dimensional ceramic nanolattices. Science 345 (6202), 1322–1326.
Mihaila, B., Knezevic, M., Cardenas, A., 2014. Three orders of magnitude improved efficiency with high-performance spectral crystal plasticity on GPU platforms. Internat. J. Numer. Methods Engrg. 97, 785–798.
Milton, G.W., 2020. Substitution of subspace collections with nonorthogonal subspaces to accelerate fast Fourier transform methods applied to conducting composites. arXiv Preprint: 2001.08289.
Mishra, N., Vondřejc, J., Zeman, J., 2016. A comparative study on low-memory iterative solvers for FFT-based homogenization of periodic media. J. Comput. Phys. 321, 151–168.
Monchiet, V., Bonnet, G., 2012. A polarization-based FFT iterative scheme for computing the effective properties of elastic composites with arbitrary contrast. Internat. J. Numer. Methods Engrg. 89, 1419–1436.
Moulinec, H., Silva, F., 2014. Comparison of three accelerated FFT-based schemes for computing the mechanical response of composite materials. Internat. J. Numer. Methods Engrg. 97, 960–985.
Moulinec, H., Suquet, P., 1994. A fast numerical method for computing the linear and nonlinear mechanical properties of composites. Comptes Rendus de L'AcadÉmie Des Sci. Paris 318, 1417–1423.
Mozaffar, M., Bostanabad, R., Chen, W., Ehmann, K., Cao, J., Bessa, M.A., 2019. Deep learning predicts path-dependent plasticity. Proc. Natl. Acad. Sci. USA 116, 26414–26420.
Ocegueda, E., Bhattacharya, K., 2021. Interaction between deformation twinning and dislocation slip in polycrystalline solids. Acta Mater. In preparation.
O'Masta, M., Deshpande, V., Wadley, H., 2014. Mechanisms of projectile penetration in dyneema® encapsulated aluminum structures. Int. J. Impact Eng. 74, 16–35.
Ortiz, M., Cuitiño, A.M., Knap, J., Koslowski, M., 2001. Mixed atomistic-continuum models of material behavior: The art of transcending atomistics and informing continua. MRS Bull. 26 (3), 216–221.
Owhadi, H., Scovel, C., Sullivan, T.J., McKerns, M., Ortiz, M., 2013. Optimal uncertainty quantification. Siam Rev. 55 (2), 271–345.
Pavliotis, G., Stuart, A., 2008. Multiscale Methods: Averaging and Homogenization. Springer Science & Business Media.
Phillips, R., 2001. Crystals, Defects and Microstructures: Modeling Across Scales. Cambridge University Press.
Pikul, J.H., Özerinç, S., Liu, B., Zhang, R., Braun, P.V., Deshpande, V.S., King, W.P., 2019. High strength metallic wood from nanostructured nickel inverse opal materials. Sci. Rep. 9 (1), 1–12.
Platzer, A., Leygue, A., Stainier, L., Ortiz, M., 2021. Finite element solver for data-driven finite strain elasticity. Comput. Methods Appl. Mech. Engrg. 379, 113756.
Schaedler, T.A., Jacobsen, A.J., Torrents, A., Sorensen, A.E., Lian, J., Greer, J.R., Valdevit, L., Carter, W.B., 2011. Ultralight metallic microlattices. Science 334 (6058), 962–965.
Schneider, M., 2020. An FFT-based method for computing weighted minimal surfaces in microstructures with applications to the computational homogenization of brittle fracture. Internat. J. Numer. Methods Engrg. 121, 1367–1387.
Schumacher, C., Bickel, B., Rys, J., Marschner, S., Daraio, C., Gross, M., 2015. Microstructures to control elasticity in 3D printing. ACM Trans. Graph. 34 (4), 1–13.
Schwartz, A.J., Kumar, M., Adams, B.L., Field, D.P., 2009. Electron backscatter diffraction in materials science. vol. 2, Springer.
Sun, X., Ariza, M.P., Ortiz, M., Wang, K., 2017. Acceleration of diffusive molecular dynamics simulations through mean field approximation and subcycling time integration. J. Comput. Phys. 350, 470–492.
Sun, X., Ariza, P., Ortiz, M., Wang, K.G., 2018. Long-term atomistic simulation of hydrogen absorption in palladium nanocubes using a diffusive molecular dynamics method. Int. J. Hydrogen Energy 43 (11), 5657–5667.
Sun, X., Ariza, M., Ortiz, M., Wang, K., 2019. Atomistic modeling and analysis of hydride phase transformation in palladium nanoparticles. J. Mech. Phys. Solids 125, 360–383.
Sun, X., Kirchdoerfer, T., Ortiz, M., 2020. Rigorous uncertainty quantification and design with uncertain material models. Int. J. Impact Eng. 136, 103418.
Sun, X., Liu, B., Bhattacharya, K., Ortiz, M., 2021. Concurrent goal-oriented materials-by-design. arXiv preprint arXiv:2106.06074.
Topcu, U., Lucas, L.J., Owhadi, H., Ortiz, M., 2011. Rigorous uncertainty quantification without integral testing. Reliab. Eng. Syst. Saf. 96 (9), 1085–1091.
Triantafyllidis, N., Nestorović, M., Schraad, M., 2006. Failure surfaces for finitely strained two-phase periodic solids under general in-plane loading. J. Appl. Mech. 73, 505–515.
Umehara, M., Stein, H.S., Guevarra, D., Newhouse, P.F., Boyd, D.A., Gregoire, J.M., 2019. Analyzing machine learning models to accelerate generation of fundamental materials insights. Npj Comput. Mater. 5, 34.
Van Der Giessen, E., Schultz, P.A., Bertin, N., Bulatov, V.V., Cai, W., Csányi, G., Foiles, S.M., Geers, M.G., González, C., Hütter, M., et al., 2020. Roadmap on multiscale materials modeling. Modelling Simulation Mater. Sci. Eng. 28, 043001.
Vidyasagar, A., Tan, W., Kochmann, D.M., 2017. Predicting the effective response of bulk polycrystalline ferroelectric ceramics via improved spectral phase field methods. J. Mech. Phys. Solids 106, 133–151.
Vondřejc, J., Zeman, J., Marek, I., 2014. An FFT-based Galerkin method for homogenization of periodic media. Comput. Math. Appl. 68, 156–173.
Wen, M., Tadmor, E.B., 2019. Hybrid neural network potential for multilayer graphene. Phys. Rev. B 100, 195419.
Wolpert, D.H., 1996. Reconciling Bayesian and non-Bayesian analysis. In: Maximum Entropy and Bayesian Methods. Springer, pp. 79–86.
Wong, K.V., Hernandez, A., 2012. A review of additive manufacturing. Int. Sch. Res. Notices 2012.
Xiao, S., Hu, R., Li, Z., Attarian, S., Björk, K.-M., Lendasse, A., 2019. A machine-learning-enhanced hierarchical multiscale method for bridging from molecular dynamics to continua. Neural Comput. Appl. 1–15.
Yogeshvaran, R., Liu, B., Farukh, F., Kandan, K., 2020. Out-of-plane compressive response of additively manufactured cross-ply composites. J. Mech. 36 (2), 197–211.
Zheng, X., Smith, W., Jackson, J., Moran, B., Cui, H., Chen, D., Ye, J., Fang, N., Rodriguez, N., Weisgraber, T., et al., 2016. Multiscale metallic metamaterials. Nature Mater. 15 (10), 1100–1106.
Zhou, H., Bhattacharya, K., 2021. Accelerated computational micromechanics and its application to polydomain liquid crystal elastomers. p. 2010.06697, arXiv.